JOURNAL OF VIROLOGY, Apr. 2005, p. 4159–4169 Vol. 79, No. 7
0022-538X/05/$08.00+0 doi:10.1128/JVI.79.7.4159–4169.2005

Cooperative Effect of Gag Proteins p12 and Capsid during Early Events of Murine Leukemia Virus Replication

Sook-Kyung Lee,[1] Kunio Nagashima,[2] and Wei-Shau Hu[1]*

HIV Drug Resistance Program, National Cancer Institute at Frederick,[1] and SAIC-Frederick,[2] Frederick, Maryland

Received 3 September 2004/Accepted 17 November 2004

The Gag polyprotein of murine leukemia virus (MLV) is processed into matrix (MA), p12, capsid (CA), and nucleocapsid (NC) proteins. p12 affects early events of virus replication and contains a PPPY motif important for virus release. To probe the functions of p12 in the early steps of MLV replication, we tested whether p12 can be replaced by spleen necrosis virus (SNV) p18, human immunodeficiency virus type 1 p6, or Rous sarcoma virus p2b. Analyses revealed that all chimeras generated virions at levels similar to that of MLV *gag-pol*; however, none of them could support MLV vector replication, and all of them exhibited severely reduced DNA synthesis upon virus infection. Because a previously reported SNV *gag*-MLV *pol* chimera, but not the MLV hybrid with SNV p18, can support replication of an MLV vector, we hypothesized that other Gag proteins act cooperatively with p12 during the early phase of virus replication. To test this hypothesis, we generated three more MLV-based chimeras containing SNV CA, p18-CA, or p18-CA-NC. We found that the MLV chimera containing SNV p18-CA or p18-CA-NC could support MLV vector replication, but the chimera containing SNV CA could not. Furthermore, viruses derived from the MLV chimera with SNV CA could synthesize viral DNA upon infection but were blocked at a post-reverse-transcription step and generated very little two long terminal repeat circle DNA, thereby producing a phenotype similar to that of the provirus formation-defective p12 mutants. Taken together, our data indicate that when p12/p18 or CA was from different viruses, despite abundant virus production and proper Gag processing, the resulting viruses were not infectious. However, when p12/p18 and CA were from the same virus, even though they were from SNV and not MLV, the resulting viruses were infectious. Therefore, these results suggest a cooperative effect of p12 and CA during the early events of MLV replication.

Retroviral *gag* encodes the structural proteins for virion formation. The *gag* gene is first translated as a polyprotein (Gag); during or after virus assembly and release from the cells, Gag is then cleaved by the virally encoded protease (PR) into mature proteins. The cleavage of Gag polyproteins from all retroviruses except spumaviruses yields three common mature proteins: matrix (MA), capsid (CA), and nucleocapsid (NC) (26, 38, 41). Additionally, other Gag proteins are generated, but depending on the virus, they vary in number and size. For example, murine leukemia virus (MLV) *gag* encodes one additional protein (p12), whereas human immunodeficiency virus type 1 (HIV-1) *gag* encodes three additional proteins (p2, p1, and p6) (38, 41).

Gag plays important roles in virus assembly; devoid of other viral elements, Gag polyproteins are capable of assembling virus-like particles in cultured cells and in vitro (6, 7, 16, 19, 29, 42). Each domain in Gag plays distinct roles during virus assembly: MA is involved in Gag targeting to the plasma membrane, CA contains major determinants of Gag-Gag interactions that enable Gag multimerization, and NC is important in viral RNA encapsidation (38). Other domains in Gag also play important roles in assembly; for example, MLV p12 and HIV-1 p6 contain motifs, PPPY and PTAP, respectively, that interact with cellular proteins to allow efficient virus release (11, 15, 22, 31).

The cleaved, mature Gag proteins also play important roles in the early events of virus replication. CA is important in the early steps of viral infection; mutations in CA could lead to a decrease of reverse transcription products (2, 5). NC has been proposed to have nucleic acid chaperone activity; mutations in NC affect reverse transcription and efficiency of integration in vivo (4, 17, 24, 33, 47).

Other Gag proteins are also important in multiple steps of viral replication. MLV p12, as a domain in Gag, is important for virus assembly and release; as a mature protein, it plays a critical role in the early events of virus replication (46). Because of the multiple functions of p12, its mutants can have three distinct phenotypes with defects in virus release, viral DNA synthesis, or integration (46). When the PPPY motif in p12 is destroyed, MLV has defects in virus release that resemble mutants of other viruses without functional PPPY or PTAP motifs. Mutations in regions other than PPPY could result in defects in the early stages of viral infection. In some mutants, very little viral DNA synthesis is detected, indicating defects in uncoating or reverse transcription. In other mutants, full-length, newly synthesized DNA can be detected; however, these DNAs are unable to integrate or generate two long terminal repeat (2-LTR) circles, indicating defects in transport of the preintegration complex or other events leading to integration (46). Intriguingly, biochemical analyses indicate little differences in the contents of the preintegration complex between wild-type MLV and a p12 mutant with integration de-

* Corresponding author. Mailing address: HIV Drug Resistance Program, NCI-Frederick, Building 535, Room 336, Frederick, MD 21702. Phone: (301) 846-1250. Fax: (301) 846-6013. E-mail: whu@ncifcrf.gov.

fects (45). Furthermore, the wild-type and mutant complexes both have DNAs with normal processing at the 3′ termini, and the isolated preintegration complexes from both wild-type and mutant MLV can perform normal DNA integration in vitro (45). Although these results clearly revealed the importance of p12 during the early events of viral replication, the exact mechanisms of action of p12 have remained unknown.

To learn more about the roles of p12 during early events of viral replication, we have taken the approach of investigating whether a heterologous domain can replace the functions of p12. We selected three heterologous domains to be tested: p2b of Rous sarcoma virus (RSV), p6 of HIV-1, and p18 of spleen necrosis virus (SNV). Studies by Yuan and colleagues have demonstrated that the PPPY or PTAP motif of RSV or HIV-1, respectively, can replace MLV PPPY and restore virion production and infectivity (44). However, in these experiments, the rest of the p12 domain was present in the chimeras to supply its functions during early infection. Therefore, whether HIV-1 p6 or RSV p2b can replace the functions of MLV p12 during the early stages of virus infection remains unknown. We selected the p18 domain of SNV because SNV is distantly related to MLV. Although p18 has low homology to p12, it may serve similar functions during the early phase of infection.

To test whether a heterologous domain can replace the functions of p12, we have generated MLV p12 deletion mutants and replaced the p12 domain with RSV p2b, HIV-1 p6, or SNV p18. Although all three domains were able to improve virus production, none of the chimeras were infectious. We previously showed that SNV Gag can replace MLV Gag to support MLV vector replication. We therefore hypothesized that other domains of Gag are needed for the p12/p18 functions. To test this hypothesis, we generated other chimeras and examined their ability to support replication and the possible blocks during replication. Our results demonstrated the restoration of infectivity when p12/p18 and CA were from the same virus, indicating a cooperative effect between homologous p12 and CA in the early stages of viral infection.

MATERIALS AND METHODS

Plasmid construction. Standard cloning procedures were used to construct all plasmids (36). Plasmid pWZH30 (47), derived from pLGPS (28), expresses MLV *gag-pol* from a truncated MLV 5′ LTR and lacks the packaging signal and the 3′ LTR. Plasmids pNL4-3 (1) and pRD136 (27) were used as templates for HIV-1 and SNV sequences, respectively.

A cloning strategy was employed to generate mutant *gag-pol* expression constructs. Briefly, DNA fragments were generated by overlapping PCR and cloned into pWZH30 to generate various *gag-pol* expression constructs. Plasmids resulting from these procedures were characterized by restriction enzyme mapping, and regions that were generated by PCR were further examined by DNA sequencing to avoid any inadvertent mutations.

Plasmid pMΔp12 was constructed as follows. Two overlapping PCR products were independently generated using pWZH30 as the template and primer pairs P3 plus 39P and P38 plus 6P; these PCR products were gel purified and combined in an overlap extension PCR using primers P3N and 6PN. The final PCR product was digested with restriction enzymes BsrGI and ClaI, and the resulting fragment was ligated to BsrGI- and ClaI-digested pWZH30. Plasmids pMΔp12/MPY and pMΔp12/Rp2b were generated using the same strategy, except that the first two PCRs used either primer pair P3 plus 41P and P40 plus 6P (pMΔp12/MPY) or P3 plus 47P and P46/6P (pMΔp12/Rp2b).

To construct the following plasmids, three overlapping PCR products were generated. These PCR products were gel purified and combined in an additional PCR to generate a DNA fragment containing a partial hybrid *gag*. The DNA fragment was digested with BsrGI and ClaI and was cloned into pWZH30. For pMΔp12/Hp6, two PCR products were amplified using pWZH30 as the template and primer pairs P3 plus 45P and P44 plus 6P, and the third PCR product was amplified using pNL4-3 as the template and primer pair P42 plus 43P. For pMΔp12/Sp18, two PCR products were generated using pWZH30 as the template and primer pairs P3 plus 20P and P19 plus 6P, and the third PCR product was generated using pRD136 as the template and primer pair P17 plus 18P. For pM/SCA, two PCR products were generated using pWZH30 as the template and primer pairs P3 plus 4P and P5 plus 6P, and a third PCR product was generated using pRD136 as the template and primer pair P1 and 2P. For pM/SPC, two PCR products were generated using pWZH30 as the template and primer pairs P3 plus 20P and P5 plus 6P, and a third PCR product was generated using pRD136 as the template and primer pair P17 plus 2P. For pM/SPCN, two PCR products were generated using pWZH30 as the template and primer pairs P3 plus 20P and P13 plus 6P, and a third PCR product was generated using pRD136 as the template and primer pair P17 plus 14P.

Cell culture, DNA transfection, and virus infection. D17 cells are dog osteosarcoma cells permissive to amphotropic MLV infection (34). The 293T cells are human embryonic kidney cells (12). SR2-293T cells are a pool of 293T cells containing SR2 proviruses derived from the MLV-based vector pSR2 (10), which expresses the hygromycin phosphotransferase B gene (*hygro*) (20) and the green fluorescent protein gene (*gfp*) (9). Cells were maintained at 37°C with 5% CO_2 in Dulbecco's modified Eagle's medium (DMEM) supplemented with 6% calf serum (D17) or 10% fetal calf serum (293T) in the presence of penicillin (50 U/ml) and streptomycin (50 μg/ml). SR2-293T cells were transfected by the calcium phosphate precipitation method (MBS transfection kit; Stratagene) (36) with a mixture of DNA containing the *gag-pol* expression construct and pSV-a-MLV-env at a 5:1 weight ratio, respectively. Plasmid pSV-a-MLV-env expresses amphotropic MLV *env* (23).

Viruses were harvested 48 h posttransfection and filtered through a 0.45-μm-pore-size membrane (Millipore) to remove cell debris. Serial 10-fold dilutions of the virus samples were performed and used to infect D17 cells in the presence of polybrene (50 μg/ml final concentration). Infected cells were selected with hygromycin (120 μg/ml final concentration), and virus titers were determined by scoring the number of hygromycin-resistant colonies.

Western analyses, RT assay, and electron microscopy (EM) analyses. Viruses were concentrated by ultracentrifugation at 25,000 rpm for 90 min at 4°C using a TH-641 rotor (Sorvall). Viral proteins in virions or in transfected cells were examined by Western analyses using polyclonal rabbit anti-MLV-CA, anti-MLV-MA (a kind gift from the AIDS Vaccine Program, SAIC-Frederick), or anti-SNV-CA antibodies (kind gifts from Nancy Rice, National Cancer Institute-Frederick). Reverse transcriptase (RT) assays were performed using standard procedures (10, 39).

To prepare the samples for EM analyses, transfected SR2-293T cells were washed with phosphate-buffered saline, pelleted by low-speed centrifugation, and fixed in 2% glutaraldehyde in cacodylate buffer (0.1 M, pH 7.4). EM analyses were performed as previously described (40) using a Hitachi H7000 electron microscope, and images were captured by a digital camera system (Gatan).

Viral RNA and DNA analyses. Cell-free virions were harvested from transfected SR2-293T cells, and virion RNAs were isolated using established protocols (13). The amounts of encapsidated SR2 RNA were detected by quantitative real-time RT-PCR using the ABI 7700 sequence detector (Applied Biosystems). Briefly, SR2 RNA was reverse transcribed using random primers, and the resulting DNA was quantified by real-time PCR as previously described (14) using the primers and probe in the *hygro* sequences (Table 1).

To study viral DNA synthesis, filtered virus supernatant was used to infect 293T cells and DNA was isolated from target 293T cells 6 and 12 h postinfection using the QIAamp DNA Blood Mini kit (QIAGEN). Viral DNA synthesis was quantified by real-time PCR using the primers and probe sets (R-U5 and U5-Ψ) specific for viral DNA as previously described (14). In parallel experiments, the amounts of the housekeeping gene porphobilinogen deaminase (PBGD) were determined and used as an internal control to standardize DNA recovery during nucleic acid isolation procedures. Data obtained from these analyses were then standardized to the RT activity of the input virus. The sequences of the primers and probes used for real-time PCR are shown in Table 1.

For the analysis of 2-LTR circle viral DNA, total cellular DNA was isolated from target 293T cells 24 h postinfection using the QIAamp DNA Blood Mini kit. The amount of total viral DNA in each sample was determined by real-time PCR using the primer and probe set detecting the U5-Ψ region. Unless specified, the same amount of viral DNA from each sample was used as the template for PCR to detect 2-LTR circle DNA with primers SR2-2LTR-F and SR2-2LTR-R, which annealed to the 5′ end of U5 and the 3′ end of U3, respectively.

TABLE 1. Primers and probes used for real-time PCR and PCR

Primers and probes	Sequences
R-U5-forward	5′TCCCAATAAAGCCTCTTGCTG 3′
R-U5-reverse	5′ AGGAGACCCTCCCAAGGAAC 3′
R-U5-probe	5′ FAM-TTGCATCCGAATCGTGGTCTC GC-TAMRA 3′
U5-ψ-forward	5′ GCCTCTTGCTGTTTGCATCC 3′
U5-ψ-reverse	5′ GTCTCCAAATCCCGGACGA 3′
U5-ψ-probe	5′ FAM-ATCGTGGTCTCGCTGTTCCTTG GGAG-TAMRA 3′
PBGD-forward	5′ AGGGATTCACTCAGGCTCTTTCT 3′
PBGD-reverse	5′ GCATGTTCAAGCTCCTTGGTAA 3′
PBGD-probe	5′ FAM-CAGGCTTTTCTCTCCAATCTGC CGGA-TAMRA 3′
Hygro-forward	5′ ACGAGGTCGCCAACATCTTC 3′
Hygro-reverse	5′ AGCGCGTCTGCTGCTCC 3′
Hygro-probe	5′ FAM-TCTGGAGGCCGTGGTTGGCTT GTA-TAMRA 3′
SR2-2LTR-F	5′-CCGAATCGTGGTCTCGCTGTTC-3′
SR2-2LTR-R	5′-GCTGTTCCATCTGTTCCTGACC-3′

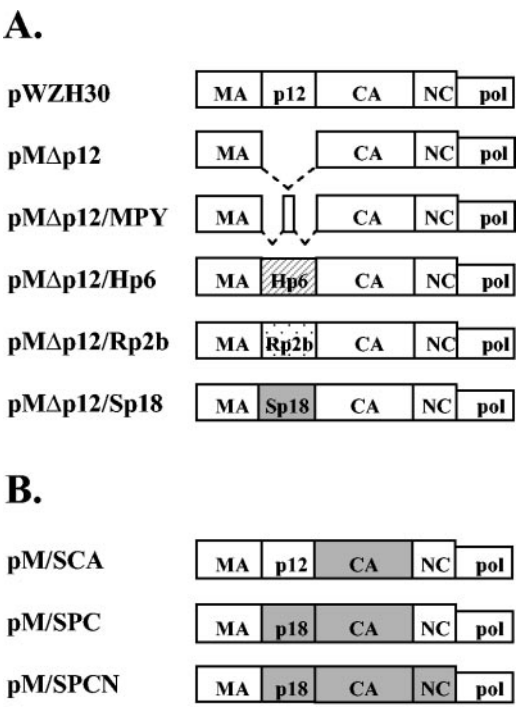

FIG. 1. General structures of the MLV-based *gag-pol* expression constructs used to study the functions of p12. (A) Wild-type MLV *gag-pol* expression construct and its derivatives containing a deletion or substitution of the p12 domain. (B) Chimeric MLV-based *gag-pol* expression constructs containing CA and other domains from SNV. Open boxes, MLV-derived sequences; shaded boxes, SNV-derived sequences; hatched box, HIV-1 p6; stippled box, RSV p2b; dashed line, deleted region.

RESULTS

Generation and examination of MLV-based *gag-pol* expression constructs containing p12 mutations or replacements. MLV and SNV are both members of the gammaretroviruses, and functional chimeras can be generated from these two viruses (8). Therefore, we hypothesized that the multiple functions of p12 can be replaced by an analogous domain in SNV, p18. Similar to MLV p12, SNV p18 is located between MA and CA and contains a PPPY motif. When the PPPY motif was destroyed, SNV virions had a tethered morphology similar to that of other viruses with a PPPY or PTAP mutation (S.-K. Lee and W.-S. Hu, unpublished data). We also hypothesized that the p6 domain of HIV-1 and the p2b domain of RSV, which respectively contain a PTAP or PPPY motif, are from evolutionarily more distant viruses, and therefore they are far less likely to be able to replace the function of p12 during the early stages of virus infection.

To probe the functions of p12 and to test our hypothesis, we generated five MLV-derived *gag-pol* expression constructs that contained mutations or replacements in p12 (Fig. 1A) based on pWZH30. Because pWZH30 expresses MLV *gag-pol* from a truncated MLV LTR and does not contain most of the MLV packaging signal, its RNA cannot be efficiently packaged by MLV proteins. However, proteins generated by pWZH30 can efficiently package MLV vector RNAs. In pMΔp12, the p12 domain was deleted except for the N- and C-terminal six amino acids to preserve the proteolytic cleavage sites. A DNA fragment encoding the MLV PPPY motif and flanking residues (LLTEDPPPYRDPR) was inserted into pMΔp12 to generate pMΔp12/MPY (Fig. 1A). Similarly, DNA fragments containing HIV-1 p6, RSV p2b, or SNV p18 sequences were inserted into pMΔp12 to generate pMΔp12/Hp6, pMΔp12/Rp2b, or pMΔp12/Sp18, respectively (Fig. 1A).

To examine the properties of virions generated by these *gag-pol* expression constructs, various *gag-pol* expression constructs were transiently transfected into SR2-293T cells along with pSV-a-MLV-env, which expresses amphotropic MLV Env. SR2-293T cells are a pool of 293T cells containing proviruses derived from pSR2 (10), an MLV-based vector that contains *cis*-acting elements essential for viral replication and encodes *hygro* and *gfp* instead of viral proteins. Culture supernatants were collected 48 h after transfection and were divided into two aliquots, one for biochemical studies, including Western analyses and RT assays, and the other for infection of D17 cells to determine virus titer. Infected D17 cells were selected with hygromycin, and the SR2 virus titers were determined by the number of hygromycin-resistant colonies. In these analyses, SR2-293T cells were transfected with only pSV-a-MLV-env as a negative control. Viral protein expression in the transfected cells was examined using cell lysates harvested at the time of virus collection.

Domains from heterologous viruses restore virion production but not infectivity. Western analyses were performed to examine the expression of viral proteins in the transfected cells and cell-free supernatants. Representative analyses are shown in Fig. 2. Anti-MLV CA antibody was used to detect viral proteins in cell lysates, whereas both anti-MLV CA and anti-MLV MA antibodies were used to detect viral proteins in the cell-free supernatants. All constructs expressed Gag precursor proteins in transfected cells (Fig. 2A). As expected, compared with pWZH30-transfected cells, pMΔp12-transfected cells released reduced amounts of virions into the supernatants (Fig. 2B). However, cells transfected with other *gag-pol* expression constructs containing various late domain motifs released virus particles into the culture supernatants at levels similar to that of pWZH30 (Fig. 2B). In multiple experiments, virions derived

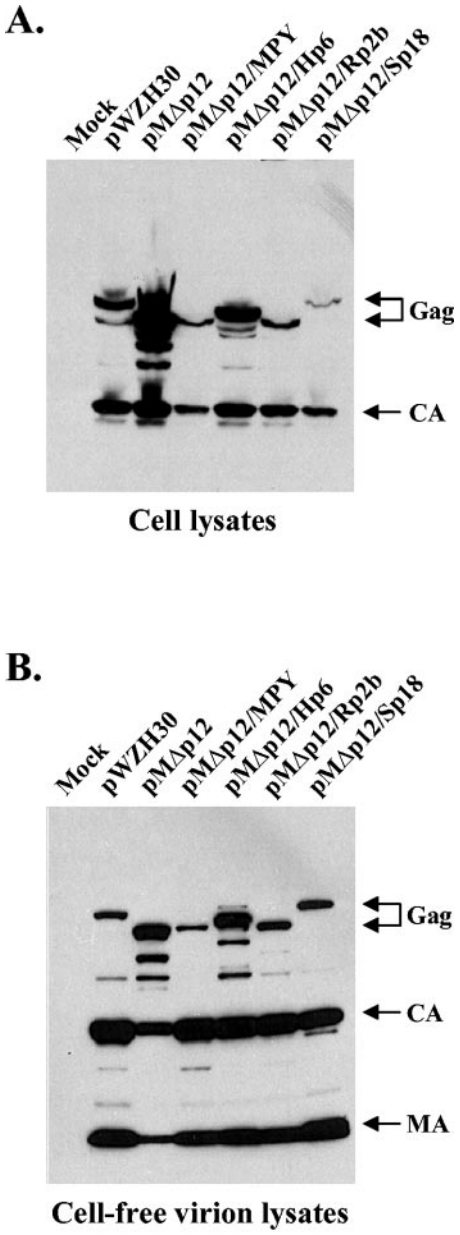

FIG. 2. Western analyses of wild-type and mutant MLV *gag* gene products in transfected cells (A) and cell-free virions (B). Anti-MLV CA antibody was used to detect *gag* gene products in transfected cell lysates, whereas both anti-MLV CA and anti-MLV MA antibodies were used to detect *gag* gene products in virion lysates.

from pMΔp12 or pMΔp12/Hp6 had more unprocessed Gag or processing intermediates than viruses derived from pWZH30, suggesting that these mutants have processing defects (Fig. 2B). Virions derived from pMΔp12/MPY, pMΔp12/Rp2b, or pMΔp12/Sp18 had low levels of unprocessed Gag or Gag intermediates, generally within the same range of those from pWZH30 in various experiments, suggesting that these mutants had few if any processing defects (Fig. 2B).

To investigate whether virions containing domains from heterologous viruses were infectious, we also examined the ability of these *gag-pol* expression constructs to support the replication of the MLV vector SR2. Virus titers generated from three sets of independent experiments are shown in Table 2. As we hypothesized, viruses from pMΔp12-, pMΔp12/MPY-, pMΔp12/Hp6-, or pMΔp12/Rp2b-transfected cells did not generate significant SR2 virus titers; however, viruses from pMΔp12/Sp18-transfected cells also did not generate significant SR2 titers. These data indicated that replacing p12 with domains from other viruses, including SNV p18, did not restore the functions of MLV p12 during virus replication.

TABLE 2. Virus titers generated by wild-type and mutant viruses

Construct	Virus titer[a]
pWZH30	$(6.6 \pm 0.3) \times 10^5$
pMΔp12	$(2.7 \pm 0.4) \times 10^0$
pMΔp12/MPY	$(4.8 \pm 1.3) \times 10^1$
pMΔp12/Hp6	$< 1 \times 10^0$
pMΔp12/Rp2b	$(4.3 \pm 1.3) \times 10^1$
pMΔp12/Sp18	$(4.5 \pm 1.1) \times 10^0$
pM/SCA	$(1.5 \pm 0.1) \times 10^1$
pM/SPC	$(4.9 \pm 1.3) \times 10^4$
pM/SPCN	$(2.8 \pm 0.6) \times 10^4$

[a] Virus titers are shown as CFU/ml (mean ± standard error). The results were summarized from three sets of independent experiments.

Other Gag domains from SNV are needed to restore the virus infectivity of pMΔp12/Sp18. In a previous report, we demonstrated that the MLV/SNV chimeric *gag-pol* construct pSNVgag, which encodes SNV *gag* and MLV *pol*, can generate infectious virions (8). In pMΔp12/Sp18, MLV p12 was replaced with SNV p18; this substitution restored virus production but not infectivity. Constructs pSNVgag and pMΔp12/Sp18 differ in the origins of the MA, CA, and NC domains. We hypothesized that other domains of Gag are important to p12 functions during the early events of virus infection. Of the different domains of Gag, the likely candidates are CA and NC, because MLV CA is present in the preintegration complexes (3, 35) and NC plays important roles during reverse transcription (17, 18, 47). To test this hypothesis, we generated three other MLV-based chimeras containing different Gag domains from SNV (Fig. 1B). Constructs pM/SCA, pM/SPC, and pM/SPCN have SNV CA, SNV P18-CA, and SNV P18-CA-NC replacing their MLV counterparts, respectively.

The expression and release of the viral proteins from these chimeras were examined by Western analyses using various combinations of anti-SNV CA, anti-MLV CA, and anti-MLV MA antibodies. Representative Western analyses are shown in Fig. 3. All three chimeric mutants were expressed in the transfected cells (data not shown) and were able to produce cell-free virions. However, compared with the wild-type MLV Gag/Gag-Pol, the amounts of virions released from these three chimeras were reduced, as indicated by the lower intensity of the MA bands (Fig. 3) and consistently lower RT activities (data not shown). Additionally, virions derived from pM/SPCN had defects in Gag processing (Fig. 3B).

We also examined whether virions generated by these chimeras were infectious. Data from three sets of independent experiments are summarized in Table 2. Viruses derived from pM/SCA generated viral titers that were comparable to those from pMΔ12/Sp18, both of which were four logs lower than the titers generated by pWZH30-derived viruses. In contrast, viruses derived from pM/SPC had much higher titers (approxi-

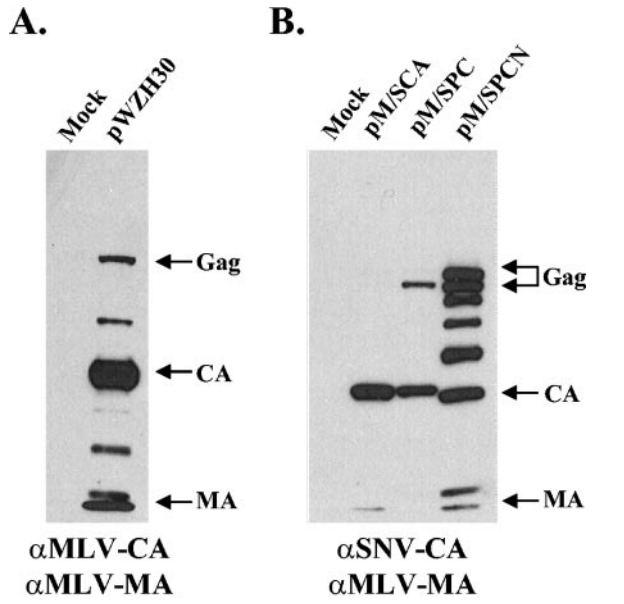

FIG. 3. Western analyses of cell-free virions harvested from cells transfected with wild-type MLV (A) or MLV/SNV chimeric *gag-pol* expression constructs (B). Anti-MLV MA and anti-MLV CA antibodies were used in the Western analysis shown in panel A, whereas anti-MLV MA and anti-SNV CA antibodies were used for panel B.

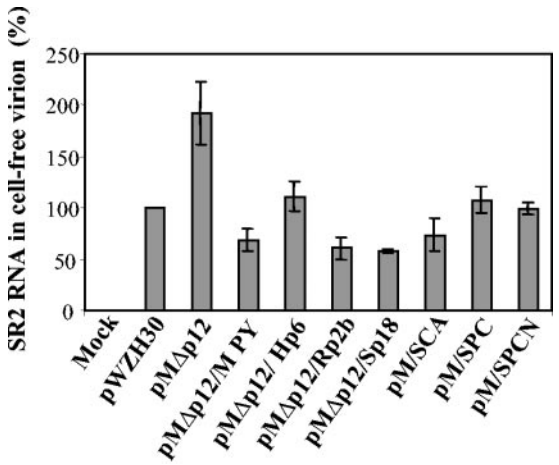

FIG. 4. Quantitation of MLV vector RNA encapsidated in cell-free virions. Levels of MLV vector SR2 RNA encapsidated in the cell-free virions derived from various *gag-pol* expression constructs were determined by real-time RT-PCR and normalized to the RT activity of the input virus. For direct comparison, the amount of RNA encapsidated by virions derived from wild-type MLV (pWZH30) was set as 100%. Data from three independent experiments are summarized and are shown as means ± standard errors.

mately 10^4 CFU/ml). When standardized to the RT activity, viruses produced from pM/SPC had infectivity similar to that from pWZH30. Viruses derived from pM/SPCN also generated high viral titers (in the range of 10^4 CFU/ml). Interestingly, the observed Gag-processing defects in pM/SPCN-derived viruses did not eliminate the infectivity (Fig. 3B, Table 2). These results indicated that virus infectivity was restored when both SNV p18 and CA were present in the Gag.

Virions derived from wild-type or mutant *gag-pol* expression constructs can efficiently encapsidate MLV vector RNA. Although most of the eight *gag-pol* expression constructs we tested did not have severe defects in virus production, only two constructs produced virions with high infectivity. Therefore, the other mutants had blocks elsewhere in the viral replication cycle. A substantial portion of the Gag polyprotein was modified in many mutant constructs; it is possible that the resulting proteins do not package SR2 RNA efficiently, thereby causing the loss of virus infectivity. Using a previously described quantitative real-time RT-PCR assay (14), we measured the amounts of SR2 vector RNA encapsidated in the cell-free virions. These measurements were standardized to RT activity, and the data summarized from three independent sets of experiments are shown in Fig. 4. Our analyses demonstrated that virions derived from all of the aforementioned mutants were able to package SR2 RNA efficiently, within twofold of that of pWZH30-derived virions. Therefore, the loss of infectivity in these mutant virions was not caused by the lack of SR2 RNA packaging in the viral particles. Additionally, these data also suggest that the p12 domain does not contribute to the specificity of virion RNA, which is consistent with the results from Yuan and colleagues (46).

Analyses of reverse transcription in cells infected with viruses derived from mutant *gag-pol* expression constructs. Because virions derived from various *gag-pol* expression constructs do not have a defect in viral RNA encapsidation, we examined reverse transcription products generated after infection to identify possible blocks in the step(s) of viral replication. Virions were harvested from transfected SR2-293T cells and used to infect 293T cells; human cells were used as target cells in these experiments to avoid the possibility of detecting MLV-related endogenous sequences, which would complicate our analyses. DNA samples were isolated from infected cells 6 and 24 h postinfection and then were analyzed by real-time PCR using primer and probe sets specifically detecting R-U5, U5-Ψ, or PBGD sequences. PBGD is a human housekeeping gene, and it serves as a control for DNA recovery during the isolation procedures. DNA samples containing equal copies of PBGD were used in the real-time PCR analyses, and the results obtained were normalized to the RT activity of the virus used to infect the target cells. For direct comparison of the efficiency of reverse transcription, in each set of experiments the copy number of viral DNA detected from cells infected with pWZH30-derived viruses was defined as 100%.

Data summarized from three sets of independent experiments are shown in Fig. 5. Detection of R-U5 DNA revealed that most of the viruses derived from mutant *gag-pol* expression constructs that failed to generate significant vector titers had a block in reverse transcription. For example, relative to cells infected with pWZH30-derived viruses, R-U5 DNA was drastically decreased (10- to 200-fold) in cells infected with viruses derived from pMΔp12, pMΔp12/MPY, pMΔp12/Hp6, pMΔp12/Rp2b, or pMΔp12/Sp18. In contrast, viruses that generated significant titers, such as those derived from pM/SPC or pM/SPCN, synthesized R-U5 efficiently. One exception was pM/SCA-derived viruses, which had a 10,000-fold decrease in viral titer (Table 2) but synthesized R-U5 DNA relatively efficiently, with a threefold decrease relative to pWZH30-derived viruses (Fig. 5).

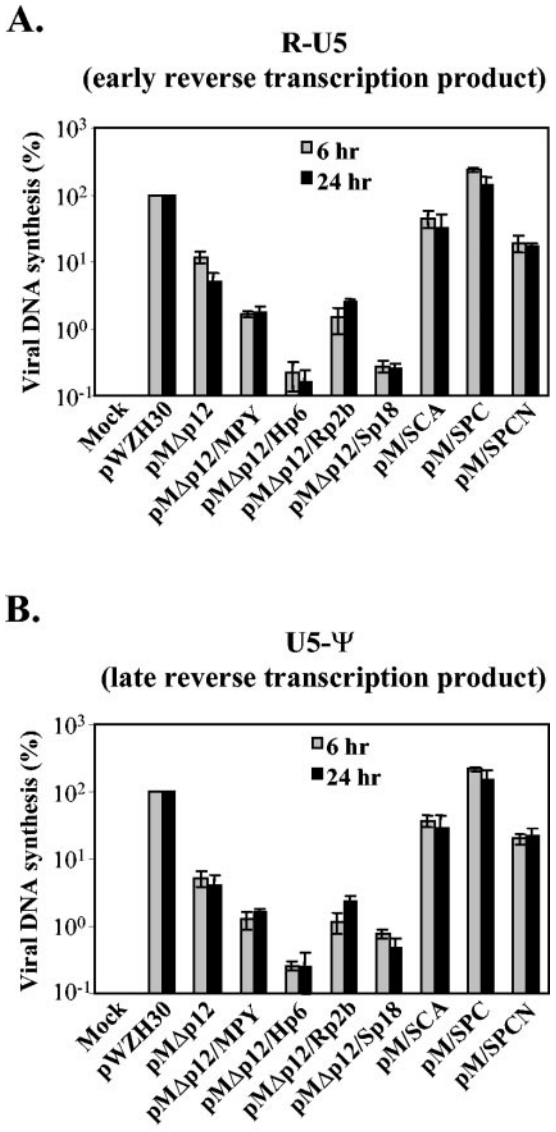

FIG. 5. Analyses of viral DNA synthesis in 293T cells infected with viruses derived from wild-type or mutant *gag-pol* expression constructs. (A) Synthesis of early reverse transcription product R-U5. (B) Synthesis of late reverse transcription product U5-Ψ. Real-time PCR was performed using primer and probe sets specific to R-U5, U5-Ψ, or PBGD sequences. PBGD quantitation served as a standard to control for variation in DNA recovery. For direct comparison, the amount of viral DNA detected from wild-type MLV was set as 100%. Data from three independent experiments are summarized and shown as means ± standard errors.

Analyses of early reverse transcription products revealed a similar trend at both 6 and 24 h postinfection, suggesting that the decreased R-U5 DNA in certain mutants was likely to be caused by blocks prior to synthesis of R-U5 rather than by delay in reverse transcription or degradation of reverse transcription products. Data from the analyses of the late reverse transcription product (U5-Ψ DNA; Fig. 5B) resembled those from the early reverse transcription products (Fig. 5A). These data suggest that once R-U5 was synthesized, the continuing synthesis of the minus-strand DNA and plus-strand DNA transfer could proceed efficiently; therefore, the blocks were likely to be at the very early steps of infection prior to or during the initiation of reverse transcription.

Mutation in the PPPY motif of p12 can interfere with the cleavage of MLV envelope transmembrane protein from p15E to the mature form p12E and can affect viral infectivity, most likely via blocks in virus entry (46). Because this cleavage defect can be rescued by inserting a functional late domain motif elsewhere in Gag (44), we do not expect our mutants to have defects in virus entry caused by p15E processing. To ensure that the reverse transcription defects in many mutant viruses were not due to blocks in virus entry, we also examined the efficiency of reverse transcription using viruses pseudotyped with vesicular stomatitis virus protein G (43). Results from real-time PCR analyses (data not shown) were similar to those shown in Fig. 5, suggesting that the step(s) of virus replication beyond entry were blocked.

pM/SCA-derived viruses exhibit a block in the formation of 2-LTR circle DNA. One of the p12 mutation phenotypes is a defect in the formation of integrated proviruses (46). Mutant viruses with this phenotype could synthesize full-length viral DNA relatively efficiently but failed to form provirus or 2-LTR circle DNA (46). Analyses of the reverse transcription products revealed that cells infected with pM/SCA-derived viruses had sufficient early and late reverse transcription products, although these viruses did not generate significant vector titers. These results were reminiscent of p12 mutants with provirus formation defects and led us to investigate whether pM/SCA-derived viruses also encountered blocks in the formation of 2-LTR circle DNA.

To investigate whether the reverse-transcribed DNA can form 2-LTR circles, we isolated total DNA 24 h postinfection. The amounts of viral DNA in these samples were determined by real-time PCR quantitation of the U5-Ψ sequences. Unless specified, DNA containing the same copy number of U5-Ψ sequences was used as the template in the PCR analyses to detect 2-LTR circle DNA with primers annealed to U5 (forward primer) or U3 (reverse primer). The resulting DNA products were analyzed by gel electrophoresis and visualization of ethidium bromide-stained DNA fragments. A representative analysis is shown in Fig. 6. PCR analyses of DNA isolated from cells infected with pWZH30-derived viruses are shown in Fig. 6A, with decreasing amounts of DNA as the template for PCR to illustrate the sensitivity of the assay, whereas PCR analyses of the wild-type and mutant viruses are shown in Fig. 6B. Similar to the studies by Yuan and colleagues (46), DNA from cells infected with pMΔp12-derived viruses contained significantly reduced amounts of 2-LTR circle DNA. Not surprisingly, 2-LTR circle DNA was generated in cells infected with pM/SPC-derived viruses, which were able to generate significant viral titers, at efficiencies similar to those from pWZH30. PCR analyses revealed that DNA from cells infected with pM/SCA-derived viruses had significantly reduced 2-LTR circle DNA, approximately 80-fold less, compared with those from pWZH30. These data indicated that pM/SCA also had a block in the post-reverse transcription step, and this CA chimera shared a similar phenotype with the provirus formation-defective p12 mutants.

EM analyses of virions generated from the mutant *gag-pol* expression constructs. Deletion of the p12 domain of MLV

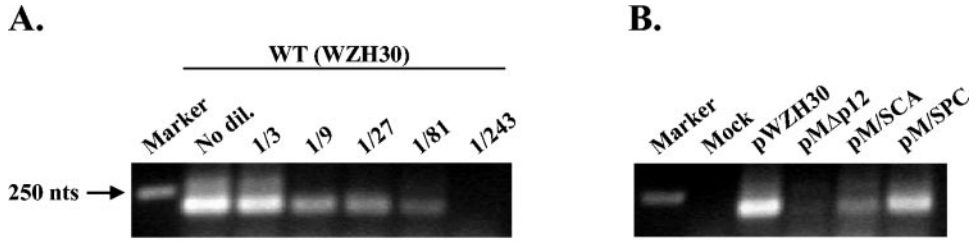

FIG. 6. Analyses of 2-LTR circle DNA in 293T cells infected with virions derived from wild-type (WT) (A) or wild-type or mutant *gag-pol* expression constructs (B). DNA was isolated from infected cells 24 h postinfection, and the amounts of viral DNA in these samples were quantified by detecting U5-Ψ sequences. Unless specified in the dilution (dil.) studies in panel A, samples containing equal amounts of viral DNA were used as the template for PCR analyses to detect 2-LTR circle DNA. nts, nucleotides.

Gag had been shown to cause drastic morphological change in the virions (44); virion-like particles had tube-like structures rather than spherical structures. In several *gag-pol* expression constructs that we generated, the p12 domain was deleted and a heterologous domain was inserted. To examine the effects of the chimeric Gag with a replaced domain on the morphology of the virions, we performed EM studies; some of the representative images are shown in Fig. 7.

EM analyses revealed that pWZH30-derived virions generated spherical structures (Fig. 7A), whereas pMΔp12 mostly generated tube-like structures having an even width (Fig. 7B); these results were consistent with previous reports (44). Particles derived from pMΔp12/MPY had various morphologies; some were spherical and others appeared to have several spherical structures fused together, creating elongated structures (Fig. 7C). The tube-like structure (Fig. 7B) had a mostly even width throughout the structure; in contrast, the elongated structure (Fig. 7C) often had indentations (or segmentations), creating the appearance of several spherical structures fused together (or structures that were unable to separate). Some elongated structures could be observed in pMΔp12 samples. Particles derived from pMΔp12/Hp6 often exhibited elongated structures or spherical structures tethered to one another (Fig. 7D). Particles generated by pMΔp12/Rp2b also had varied phenotypes, some with a spherical morphology and others with elongated structures or tethered spherical structures (Fig. 7E). Particles generated by pMΔp12/Sp18 had a spherical morphology (Fig. 7F); similarly, spherical structures were observed within virions derived from pM/SCA, pM/SPC, or pM/SPCN (Fig. 7G to I). These results indicated that the morphology of the virions generated from pMΔp12, pMΔp12/MPY, pMΔp12/Hp6, or pMΔp12/Rp2b is not similar to that of the wild-type viruses. Deletion of the MLV p12 domain caused assembly and release defects; these defects could not be completely corrected by placing the HIV-1 p6 or RSV p2b domain in the location of p12, although these two heterologous domains contained a functional PTAP or PPPY motif.

DISCUSSION

The cooperative effect of MLV p12 and CA on the early events of virus infection. In this study, we report a cooperative effect of p12 and CA in viral infectivity by characterizing MLV-based chimeras with Gag domains replaced by heterologous counterparts. Replacing MLV p12 with SNV p18 or MLV CA with SNV CA resulted in two single chimeras with very low virus infectivity. However, the double chimera, with both MLV p12 and CA replaced by their SNV counterparts, had an infectivity similar to that of the wild-type MLV. Considering that p12 and CA constitute a major portion of the MLV Gag polyprotein, it would not be surprising if the cooperative effect were on virus production or RNA encapsidation. For example, it is possible that proper Gag folding was disrupted in single (p12 or CA) chimeras but was restored in the double chimera, hence generating the cooperative effect. However, both single chimeras produced ample viruses without apparent processing defects or RNA encapsidation defects. One of the chimeras, pM/SCA, could efficiently synthesize viral DNA (30% of wild type). These results strongly suggest that the p12-CA cooperative effect influences the early events of virus replication rather than the late events of viral replication, such as virion production.

Replacing MLV CA with SNV CA resulted in a chimera presenting a phenotype identical to that of the p12 mutant with provirus formation defects, with efficient viral DNA synthesis and severe reduction of 2-LTR circle DNA formation. At this time, we do not know the exact mechanisms of the block in either mutant; however, an interesting possibility is that the same defects caused the disruption of viral replication in both the CA chimera and the provirus formation-deficient p12 mutant, thereby generating the same phenotype. Studies by Yuan and colleagues elegantly demonstrated that the preintegration complexes generated by wild-type MLV and p12 mutants are comparable both biochemically and in their ability to carry out the integration reaction in vitro (45). These data strongly suggest that the p12 mutants have defects in the transport of preintegration complexes. It is possible that CA also plays a role in preintegration complex transport, because CA is part of the MLV preintegration complex (3). Furthermore, the restriction factor Fv-1 targets MLV CA and blocks virus replication at a stage after reverse transcription and before integration, similar to the p12 provirus formation-deficient mutants (37). Strikingly, the MLV preintegration complexes isolated from Fv-1-restricted cells were also functional in vitro, again similar to the p12 mutant (32).

One intriguing hypothesis is that both p12 and CA are important in the proper transport of the MLV preintegration complex, which can be blocked by interference with either protein. This hypothesis can explain why our pM/SCA mutant has a phenotype similar to that of MLV p12 provirus formation-deficient mutants. It is possible that p12 and CA from

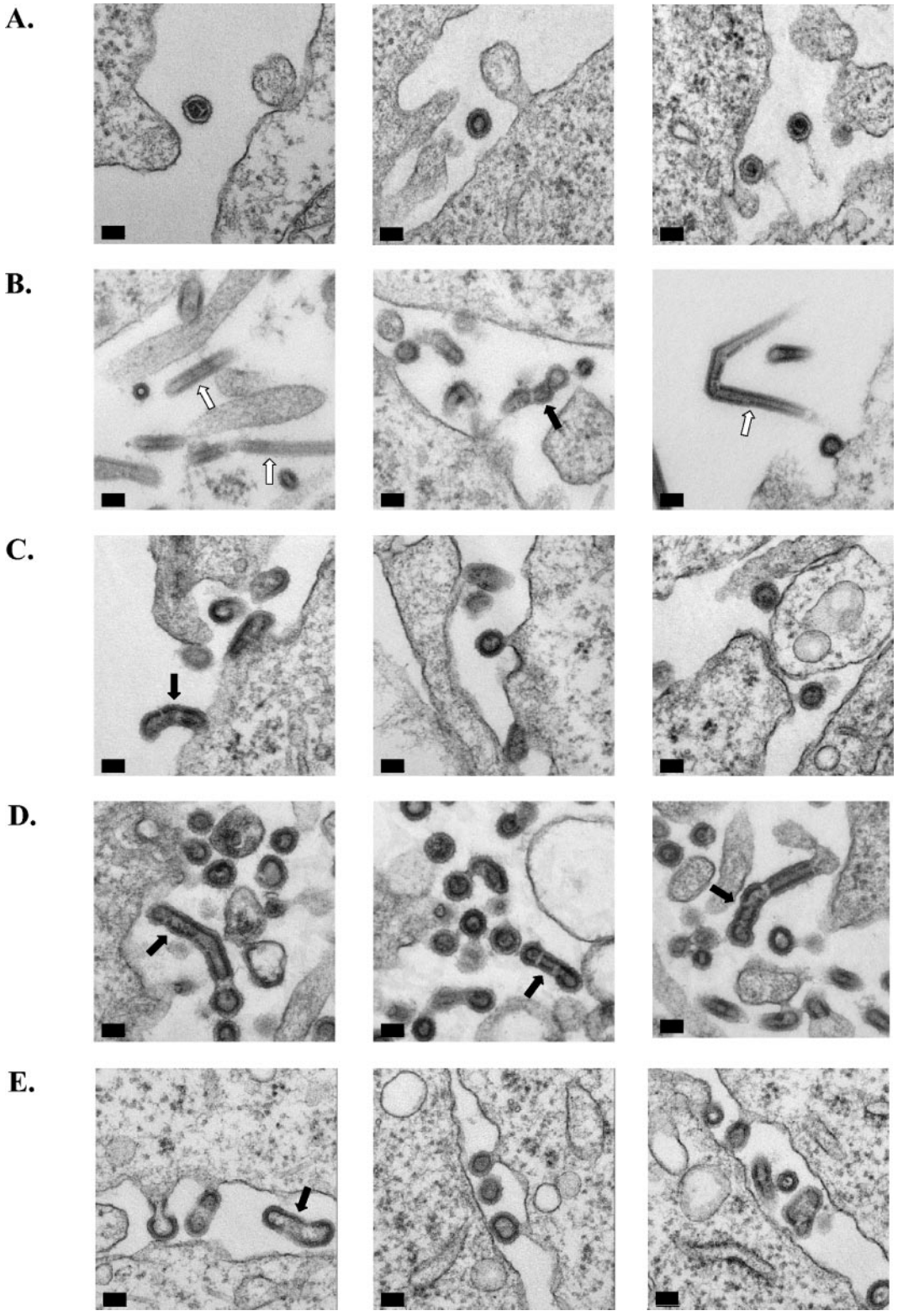

FIG. 7. EM analyses of wild-type and mutant MLV particles. Virions were derived from pWZH30 (A), pMΔp12 (B), pMΔp12/PY (C), pMΔp12/Hp6 (D), pMΔp12/Rp2b (E), pMΔp12/Sp18 (F), pM/SCA (G), pM/SPC (H), or pM/SPCN (I). The black bar in each electron micrograph indicates 100 nm. Tube-like structures are indicated by white arrows; elongated structures are indicated by solid arrows.

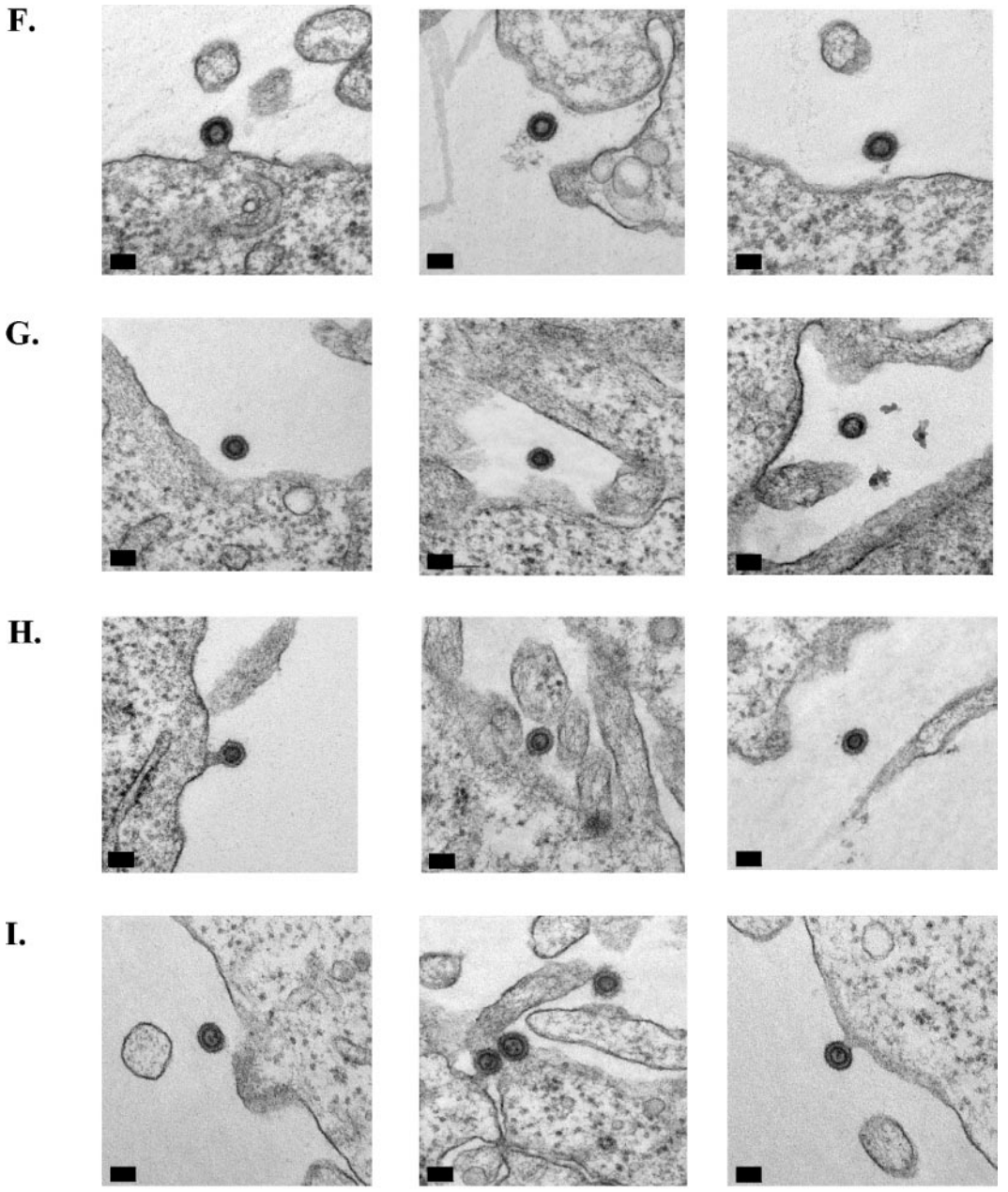

FIG. 7—*Continued*.

different viruses cannot properly direct preintegration complex transport. In this scenario, virions produced by both single chimeras (pM/SCA and pMSp18) would have low infectivity, and the virions from the double chimera (pM/SPC) would have fully restored infectivity. Although this hypothesis is attractive, further experiments are needed to better define the blocks in viral replication and the exact nature of the p12-CA cooperative effect. We do not know at this time whether p12 and CA directly interact or if both are required to form a functional preintegration complex. We also do not know whether either protein plays structural roles or more functional roles, such as recruitment of or interaction with host proteins, to direct the transport of the preintegration complex or other steps leading to provirus formation.

The roles of p12 in virion morphology, assembly, and release. It was previously shown that mutations of p12 resulted in two types of morphologically different defects in virions (44). Deletion of p12 resulted in the formation of tube-like structures, whereas destroying the PPPY motif but leaving most of p12 intact resulted in tethered particles similar to late-domain mutants from other viruses. In this report, we generated seven other mutants with modifications in p12 and/or other regions of *gag*. Preserving the MLV PPPY motif but deleting the rest of p12 or replacing p12 with HIV-1 p6 or RSV p2b rescued the

virus production (Fig. 2), but it did not completely restore defects in virus assembly and release. Virions derived from these three constructs had mixed morphologies; some particles appeared to be spherical, and others appeared to be fused to one another in elongated structures (Fig. 7C to E). It was possible that some of the spherical particles we observed in these mutants were actually from the elongated structures. However, we observed far more spherical particles from these constructs than from p12 deletion mutants (Fig. 7B), suggesting that some of the particles were likely to be spherical in nature. These results suggest that the PPPY motif or heterologous domains can partially rescue but cannot restore the wild-type virion morphology. These results enforce the notion that, in addition to the PPPY motif, other parts of p12 play a role in shaping the virion morphology. Interestingly, when we replaced p12 with SNV p18, we observed almost all spherical particles, indicating that p18 can replace the roles of p12 in assembly better than HIV-1 p6 or RSV p2b. One possible interpretation of these results is that p18 is a larger domain than p6 or p2b, therefore it provides sufficient spacing in Gag to allow proper folding and Gag interaction. It is also possible that the particular folding of Gag, and not the size of p18, determines the virion morphology.

Interestingly, a so-called shape-determinant region has been observed in the RSV p10 domain of Gag, which is located between MA and CA and adjacent to p2. Deletion of RSV p10 results in the formation of tubular-shaped virus-like particles; further mapping revealed that the C-terminal region of p10 is responsible for the shape-determinant role during virus assembly (21, 30). It is unclear whether there are regions in MLV p12 and SNV p18 that play the same shape-determinant role during virus assembly. However, the C-terminal region of MLV p12 could not replace the function of RSV p10 during RSV assembly (21). Further experimentation will be needed to characterize whether there are defined regions in MLV p12 that possess the shape-determinant function.

In this report, we demonstrated that viruses generated by various mutants and chimeric MLV gag packaged MLV vector RNA efficiently. These results suggested that MLV p12 did not play a critical role in the specific viral RNA packaging. Interestingly, RSV p10 could affect RNA packaging; mutation in RSV p10 could rescue an RNA packaging-defective NC mutant. These results suggest that RSV p10 could interact with other domains of gag and affect RNA packaging specificity (25).

In summary, results from this study further revealed the multiple roles that p12 plays during MLV replication. The cooperative effect with CA in the early phase of viral replication suggests that p12, together with another viral protein(s), mediates proper transport of the preintegration complex for integration into the host genome. Furthermore, besides the known function of the PPPY motif, other regions of p12 play structural roles during virus assembly to ensure proper morphology of the virions. Future research is needed to further understand the precise roles of p12 in the transport of preintegration complex and virion assembly.

ACKNOWLEDGMENTS

We thank Vinay Pathak for intellectual input and encouragement for this project, Anne Arthur for expert editorial help, and Vinay Pathak and Eric Freed for critical reading of the manuscript.

REFERENCES

1. **Adachi, A., H. E. Gendelman, S. Koenig, T. Folks, R. Willey, A. Rabson, and M. A. Martin.** 1986. Production of acquired immunodeficiency syndrome-associated retrovirus in human and nonhuman cells transfected with an infectious molecular clone. J. Virol. **59:**284–291.
2. **Alin, K., and S. P. Goff.** 1996. Amino acid substitutions in the CA protein of Moloney murine leukemia virus that block early events in infection. Virology **222:**339–351.
3. **Bowerman, B., P. O. Brown, J. M. Bishop, and H. E. Varmus.** 1989. A nucleoprotein complex mediates the integration of retroviral DNA. Genes Dev. **3:**469–478.
4. **Buckman, J. S., W. J. Bosche, and R. J. Gorelick.** 2003. Human immunodeficiency virus type 1 nucleocapsid zn(2+) fingers are required for efficient reverse transcription, initial integration processes, and protection of newly synthesized viral DNA. J. Virol. **77:**1469–1480.
5. **Cairns, T. M., and R. C. Craven.** 2001. Viral DNA synthesis defects in assembly-competent Rous sarcoma virus CA mutants. J. Virol. **75:**242–250.
6. **Campbell, S., and A. Rein.** 1999. In vitro assembly properties of human immunodeficiency virus type 1 Gag protein lacking the p6 domain. J. Virol. **73:**2270–2279.
7. **Campbell, S., and V. M. Vogt.** 1997. In vitro assembly of virus-like particles with Rous sarcoma virus Gag deletion mutants: identification of the p10 domain as a morphological determinant in the formation of spherical particles. J. Virol. **71:**4425–4435.
8. **Certo, J. L., T. O. Kabdulov, M. L. Paulson, J. A. Anderson, and W. S. Hu.** 1999. The nucleocapsid domain is responsible for the ability of spleen necrosis virus (SNV) Gag polyprotein to package both SNV and murine leukemia virus RNA. J. Virol. **73:**9170–9177.
9. **Chalfie, M., Y. Tu, G. Euskirchen, W. W. Ward, and D. C. Prasher.** 1994. Green fluorescent protein as a marker for gene expression. Science **263:**802–805.
10. **Cheslock, S. R., J. A. Anderson, C. K. Hwang, V. K. Pathak, and W. S. Hu.** 2000. Utilization of nonviral sequences for minus-strand DNA transfer and gene reconstitution during retroviral replication. J. Virol. **74:**9571–9579.
11. **Demirov, D. G., A. Ono, J. M. Orenstein, and E. O. Freed.** 2002. Overexpression of the N-terminal domain of TSG101 inhibits HIV-1 budding by blocking late domain function. Proc. Natl. Acad. Sci. USA **99:**955–960.
12. **DuBridge, R. B., P. Tang, H. C. Hsia, P. M. Leong, J. H. Miller, and M. P. Calos.** 1987. Analysis of mutation in human cells by using an Epstein-Barr virus shuttle system. Mol. Cell. Biol. **7:**379–387.
13. **Fu, W., R. J. Gorelick, and A. Rein.** 1994. Characterization of human immunodeficiency virus type 1 dimeric RNA from wild-type and protease-defective virions. J. Virol. **68:**5013–5018.
14. **Fu, W., and W. S. Hu.** 2003. Functional replacement of nucleocapsid flanking regions by heterologous counterparts with divergent primary sequences: effects of chimeric nucleocapsid on the retroviral replication cycle. J. Virol. **77:**754–761.
15. **Garrus, J. E., U. K. von Schwedler, O. W. Pornillos, S. G. Morham, K. H. Zavitz, H. E. Wang, D. A. Wettstein, K. M. Stray, M. Cote, R. L. Rich, D. G. Myszka, and W. I. Sundquist.** 2001. Tsg101 and the vacuolar protein sorting pathway are essential for HIV-1 budding. Cell **107:**55–65.
16. **Gheysen, D., E. Jacobs, F. de Foresta, C. Thiriart, M. Francotte, D. Thines, and M. De Wilde.** 1989. Assembly and release of HIV-1 precursor Pr55gag virus-like particles from recombinant baculovirus-infected insect cells. Cell **59:**103–112.
17. **Gonsky, J., E. Bacharach, and S. P. Goff.** 2001. Identification of residues of the Moloney murine leukemia virus nucleocapsid critical for viral DNA synthesis in vivo. J. Virol. **75:**2616–2626.
18. **Gorelick, R. J., W. Fu, T. D. Gagliardi, W. J. Bosche, A. Rein, L. E. Henderson, and L. O. Arthur.** 1999. Characterization of the block in replication of nucleocapsid protein zinc finger mutants from Moloney murine leukemia virus. J. Virol. **73:**8185–8195.
19. **Gottlinger, H. G.** 2001. The HIV-1 assembly machine. Aids **15**(Suppl. 5)**:** S13–S20.
20. **Gritz, L., and J. Davies.** 1983. Plasmid-encoded hygromycin B resistance: the sequence of hygromycin B phosphotransferase gene and its expression in Escherichia coli and Saccharomyces cerevisiae. Gene **25:**179–188.
21. **Joshi, S. M., and V. M. Vogt.** 2000. Role of the Rous sarcoma virus p10 domain in shape determination of gag virus-like particles assembled in vitro and within *Escherichia coli*. J. Virol. **74:**10260–10268.
22. **Kikonyogo, A., F. Bouamr, M. L. Vana, Y. Xiang, A. Aiyar, C. Carter, and J. Leis.** 2001. Proteins related to the Nedd4 family of ubiquitin protein ligases interact with the L domain of Rous sarcoma virus and are required for gag budding from cells. Proc. Natl. Acad. Sci. USA **98:**11199–11204.
23. **Landau, N. R., K. A. Page, and D. R. Littman.** 1991. Pseudotyping with human T-cell leukemia virus type I broadens the human immunodeficiency virus host range. J. Virol. **65:**162–169.
24. **Lapadat-Tapolsky, M., C. Gabus, M. Rau, and J. L. Darlix.** 1997. Possible roles of HIV-1 nucleocapsid protein in the specificity of proviral DNA synthesis and in its variability. J. Mol. Biol. **268:**250–260.
25. **Lee, E. G., and M. L. Linial.** 2004. Basic residues of the retroviral nucleo-

capsid play different roles in gag-gag and Gag-Psi RNA interactions. J. Virol. **78:**8486–8495.
26. **Leis, J., D. Baltimore, J. M. Bishop, J. Coffin, E. Fleissner, S. P. Goff, S. Oroszlan, H. Robinson, A. M. Skalka, H. M. Temin, et al.** 1988. Standardized and simplified nomenclature for proteins common to all retroviruses. J. Virol. **62:**1808–1809.
27. **Martinez, I., and R. Dornburg.** 1995. Improved retroviral packaging lines derived from spleen necrosis virus. Virology **208:**234–241.
28. **Miller, A. D., and C. Buttimore.** 1986. Redesign of retrovirus packaging cell lines to avoid recombination leading to helper virus production. Mol. Cell. Biol. **6:**2895–2902.
29. **Morikawa, Y., T. Goto, and K. Sano.** 1999. In vitro assembly of human immunodeficiency virus type 1 Gag protein. J. Biol. Chem. **274:**27997–28002.
30. **Nandhagopal, N., A. A. Simpson, M. C. Johnson, A. B. Francisco, G. W. Schatz, M. G. Rossmann, and V. M. Vogt.** 2004. Dimeric rous sarcoma virus capsid protein structure relevant to immature Gag assembly. J. Mol. Biol. **335:**275–282.
31. **Pornillos, O., J. E. Garrus, and W. I. Sundquist.** 2002. Mechanisms of enveloped RNA virus budding. Trends Cell Biol. **12:**569–579.
32. **Pryciak, P. M., and H. E. Varmus.** 1992. Fv-1 restriction and its effects on murine leukemia virus integration in vivo and in vitro. J. Virol. **66:**5959–5966.
33. **Rein, A., L. E. Henderson, and J. G. Levin.** 1998. Nucleic-acid-chaperone activity of retroviral nucleocapsid proteins: significance for viral replication. Trends Biochem. Sci. **23:**297–301.
34. **Riggs, J. L., R. M. McAllister, and E. H. Lennette.** 1974. Immunofluorescent studies of RD-114 virus replication in cell culture. J. Gen. Virol. **25:**21–29.
35. **Risco, C., L. Menendez-Arias, T. D. Copeland, P. Pinto da Silva, and S. Oroszlan.** 1995. Intracellular transport of the murine leukemia virus during acute infection of NIH 3T3 cells: nuclear import of nucleocapsid protein and integrase. J. Cell Sci. **108**(Part 9)**:**3039–3050.
36. **Sambrook, J., E. F. Fritsch, and T. Maniatis.** 1989. Molecular cloning: a laboratory manual, 2nd ed. Cold Spring Harbor Laboratory Press, Cold Spring Harbor, N.Y.
37. **Stoye, J. P.** 1998. Fv1, the mouse retrovirus resistance gene. Rev. Sci. Technol. **17:**269–277.
38. **Swanstrom, R., and J. W. Wills.** 1997. Synthesis, assembly, and processing of viral proteins, p. 263–334. *In* J. M. Coffin, S. H. Hughes, and H. E. Varmus (ed.), Retroviruses. Cold Spring Harbor Laboratory Press, Cold Spring Harbor, N.Y.
39. **Temin, H. M., and S. Mizutani.** 1970. RNA-dependent DNA polymerase in virions of Rous sarcoma virus. Nature **226:**1211–1213.
40. **Tobin, G. J., K. Nagashima, and M. A. Gonda.** 1996. Immunologic and ultrastructural characterization of HIV pseudovirions containing Gag and Env precursor proteins engineered in insect cells. Methods **10:**208–218.
41. **Vogt, V. M.** 1997. Retroviral virions and genomes. Cold Spring Harbor Laboratory Press, Cold Spring Harbor, N.Y.
42. **Wills, J. W., and R. C. Craven.** 1991. Form, function, and use of retroviral gag proteins. AIDS **5:**639–654.
43. **Yee, J. K., A. Miyanohara, P. LaPorte, K. Bouic, J. C. Burns, and T. Friedmann.** 1994. A general method for the generation of high-titer, pantropic retroviral vectors: highly efficient infection of primary hepatocytes. Proc. Natl. Acad. Sci. USA **91:**9564–9568.
44. **Yuan, B., S. Campbell, E. Bacharach, A. Rein, and S. P. Goff.** 2000. Infectivity of Moloney murine leukemia virus defective in late assembly events is restored by late assembly domains of other retroviruses. J. Virol. **74:**7250–7260.
45. **Yuan, B., A. Fassati, A. Yueh, and S. P. Goff.** 2002. Characterization of Moloney murine leukemia virus p12 mutants blocked during early events of infection. J. Virol. **76:**10801–10810.
46. **Yuan, B., X. Li, and S. P. Goff.** 1999. Mutations altering the moloney murine leukemia virus p12 Gag protein affect virion production and early events of the virus life cycle. EMBO J. **18:**4700–4710.
47. **Zhang, W. H., C. K. Hwang, W. S. Hu, R. J. Gorelick, and V. K. Pathak.** 2002. Zinc finger domain of murine leukemia virus nucleocapsid protein enhances the rate of viral DNA synthesis in vivo. J. Virol. **76:**7473–7484.